[Re] Unstable modes in the four-dimensional causal-set d'Alembertian: replication and robustness

LiWeibing · Independent Researcher, China · 27 August 2026

Abstract

Aslanbeigi, Saravani, and Sorkin found that the continuum-averaged four-dimensional causal-set d'Alembertian has two nonzero complex spectral zeros and is therefore unstable under their plane-wave criterion. We reproduce that calculation from the integral representation of the spectrum. Adaptive quadrature gives

$$Z_\star = -25.3840413101 \pm 3.79522481695i,$$

and a keyhole-contour calculation gives a phase change of 4π, counting two nonzero zeros without relying on root-search seeds. The count is unchanged when the inner and outer contour radii and sampling densities are varied. We also consider the first nonminimal operator, obtained by adding a fifth layer. After solving the infrared constraints with $b_4 = q$, implicit differentiation yields

$$\left.\frac{dZ_\star}{dq}\right|_{q=0} = -0.242882613 + 0.036313923i.$$

Thus the unstable pair survives sufficiently small fifth-layer deformations. Numerical continuation tracks the pair over $-20 \le q \le 20$. The code, tests, pinned environment, and convergence records are supplied with the article.

Background and scope

A causal set replaces a Lorentzian spacetime by a locally finite partial order. For a causal set obtained by Poisson sprinkling into Minkowski spacetime, the order records causal precedence and the number of elements records spacetime volume. Scalar d'Alembertians constructed from order intervals are retarded and Lorentz invariant, but necessarily nonlocal. Their sprinkling averages define continuum integral operators that approach the ordinary d'Alembertian in the infrared.

The spectral analysis of Aslanbeigi et al. (2014) showed that the minimal operator is stable in two dimensions but has a conjugate pair of unstable zeros in four dimensions. The same paper introduced an infinite family of generalized operators and reported that no stable four-dimensional choice had been found. The purpose of the present calculation is narrower: to reproduce the minimal four-dimensional zero count with an independent implementation and to test how that pair responds to the single new coefficient available in the five-layer family.

Spectrum and infrared constraints

For a generalized operator with coefficients a and b_n, the four-dimensional continuum spectrum can be written as

$$\tilde{g}(Z) = a + 4\pi Z^{-1/2} \sum_{n=0}^{L} \frac{b_n}{n!} C_4^n \int_0^\infty ds, s^{4n+2} e^{-C_4 s^4} K_1(\sqrt{Z}s), \qquad C_4 = \frac{\pi}{24},$$

where $Z = \rho^{-1/2} p \cdot p$. We use the principal branches of $\sqrt{Z}$ and K_1, so the spectrum has a branch cut on the negative real axis. Recovery of $\tilde{g}(Z) \sim -Z$ at small Z requires

$$\sum_n \frac{b_n}{n!}\Gamma\left(n+\frac{1}{2}\right)=0, \qquad \sum_n \frac{b_n}{n!}\Gamma(n+1)=0,$$
$$\sum_n \frac{b_n}{n!}\Gamma\left(n+\frac{3}{2}\right)=0,$$

together with the normalization condition

$$\sum_n \frac{b_n}{n!}\Gamma\left(n+\frac{3}{2}\right)\psi\left(n+\frac{3}{2}\right)=-\frac{64}{\pi}\left(\frac{\pi}{24}\right)^{3/2}.$$

The remaining coefficient is

$$a=-3\sum_n b_n\psi(n+1).$$

For $L=3$ these equations have the unique solution

$$(a,b_0,b_1,b_2,b_3)=\frac{1}{\sqrt{6}}(-4,4,-36,64,-32),$$

which agrees with Aslanbeigi et al. (2014). The largest residual in our numerical evaluation of the four constraints is 6.4×10^{-15}.

Numerical calculation

The integral is evaluated after summing the layer polynomial inside the integrand. Evaluating each layer separately is algebraically equivalent, but near the infrared it loses precision through cancellation. The real and imaginary parts of the combined integrand are integrated independently on $[0,\infty)$ with adaptive quadrature. A two-dimensional nonlinear solve then locates the zero in the upper half-plane.

The number of zeros is checked independently with the argument principle. The contour is a counter-clockwise keyhole around the negative-real-axis branch cut. A clockwise inner circle removes the known zero at $Z=0$. If $\tilde{g}$ is nonzero on the contour, the number of enclosed nonzero zeros is

$$N=\frac{1}{2\pi}\Delta\arg\tilde{g}.$$

The implementation records the minimum of $|\tilde{g}|$ on each contour segment, rather than inferring the winding number across a point where the spectrum might vanish.

Replication results

The upper-half-plane root is

$$Z_\star=-25.38404131011211+3.79522481694451i, \qquad |\tilde{g}(Z_\star)|=2.4\times10^{-14}.$$

Complex conjugation supplies the second root. For the standard contour with outer radius $R=300$ and inner radius $\epsilon=0.03$, the four contour segments give a total phase change

$$\Delta\arg\tilde{g}=12.566370614359169,$$

which is 4π to the displayed precision and therefore gives $N=2$.

R	ϵ	**Lip samples**	**Circle samples**	**Winding number**
100	0.10	251	201	2.000000000000000
300	0.10	301	241	2.000000000000000

		Lip samples	Circle samples	Winding number
300	0.03	401	321	1.999999999999999
1000	0.03	501	401	1.999999999999999
300	0.01	501	401	2.000000000000000

The smallest value of $|\tilde{g}|$ on any contour in this table is 9.8×10^{-3}. The zero count is consequently well separated from a contour crossing at the tested resolutions.

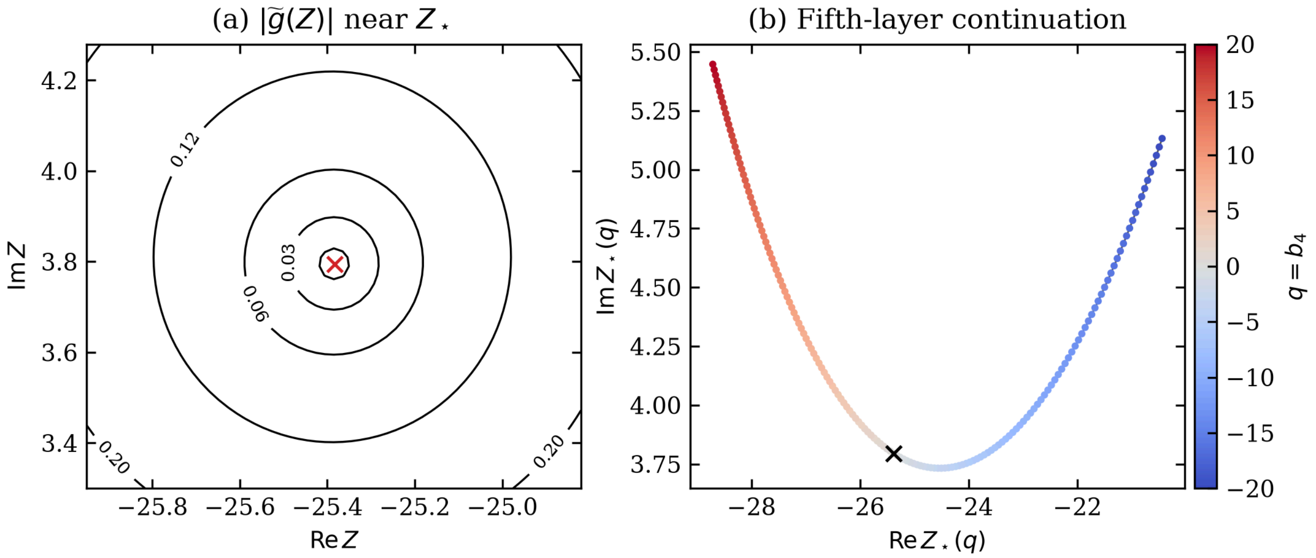

Figure 1. Left: contours of $|\tilde{g}(Z)|$ around the upper-half-plane zero. Right: continuation of the same zero through the five-layer family; colour denotes $q = b_4$. The black cross marks $q = 0$.

Five-layer deformation

The first nonminimal case has $L = 4$. Setting $b_4 = q$ leaves four coefficients to be fixed by the four infrared constraints. Differentiating that linear system gives

$$\frac{d(b_0, b_1, b_2, b_3, b_4)}{dq} = \left(\frac{3}{64}, -\frac{47}{64}, \frac{37}{16}, -\frac{21}{8}, 1\right), \qquad \frac{da}{dq} = -\frac{1}{64}.$$

Because the spectrum depends linearly on these coefficients, a simple zero obeys

$$\frac{dZ_\star}{dq} = -\frac{\partial_q \tilde{g}}{\partial_Z \tilde{g}}.$$

At the minimal operator we find

$$\partial_Z \tilde{g}(Z_\star) = 0.0774299961 + 0.2836963044i,$$

which is nonzero, and hence the unstable root continues uniquely for sufficiently small $|q|$. Direct continuation in steps of $\Delta q = 0.5$ gives

$$Z_\star(-20) = -20.4385393668 + 5.1322768858i,$$

$$Z_\star(20) = -28.7101498048 + 5.4472097454i.$$

The pair remains off the branch cut throughout this interval. This calculation does not exclude a collision, a branch-cut crossing, or escape to infinity at larger $|q|$, and it says nothing about families with more than five layers.

Discussion

The root location and the argument-principle count reproduce the central four-dimensional stability result of Aslanbeigi et al. (2014) with an implementation written from the published formulas. The five-layer calculation adds a local statement that does not follow from merely observing the root at $q = 0$: since $\partial_Z \tilde{g}(Z_\star) \neq 0$, a small change of the extra layer coefficient cannot remove the instability. The finite continuation shows that this persistence extends well beyond the perturbative neighbourhood examined by the implicit-function theorem.

Our calculation concerns the continuum-averaged scalar operator in flat spacetime. It does not address fluctuations between individual sprinklings, curvature, interactions, or boundary conditions. Nor does it settle how the complex modes should be treated in the quantum theory. In particular, the Wheeler-propagator prescription considered by Belenchia et al. (2015) may remove these modes from asymptotic states while leaving questions about energy positivity. Those issues lie outside the present replication.

Reproducibility

The repository contains the spectrum implementation, scripts for the root, contour, and continuation calculations, regression tests, the plotting script, and pinned Python dependencies. The main results can be reproduced with

```
python -m pip install -r requirements.txt
python reproduce.py
python -m unittest -v test_gcb4.py
```

The package was also run in a fresh Python 3.12 virtual environment containing only the pinned dependencies. All four tests passed, and the root, winding number, and five-layer derivative agreed with the archived reference output.

References

Aslanbeigi, S., Saravani, M., & Sorkin, R. D. (2014). Generalized causal set d'Alembertians. *Journal of High Energy Physics*, 2014(6), 24. https://doi.org/10.1007/JHEP06(2014)024

Belenchia, A., Benincasa, D. M. T., & Liberati, S. (2015). Nonlocal scalar quantum field theory from causal sets. *Journal of High Energy Physics*, 2015(3), 36. https://doi.org/10.1007/JHEP03(2015)036

Acknowledgements and disclosure

OpenAI Codex was used to assist with portions of the code and prose. The human author is responsible for the calculations, interpretation, and final text.